PROCEEDINGS OF SCIENCE

Entanglement islands and black holes deformations

Dmitry Ageev[a,*]

[a] *Steklov Mathematical Institute, Russian Academy of Sciences*
Gubkin str. 8, Moscow, Russian Federation

E-mail: ageev@mi-ras.ru

In this paper, we consider the entanglement entropy and entanglement islands in the two-sided generalization of the Schwarzschild black hole in a cavity. We find that entanglement entropy saturates at some constant value thus for some values avoiding information paradox (in the Page curve formulation). Also we find, that inclusion of the entanglement islands leads to a universal effect induced by the boundary presence, which we call “blinking island". For some time the entanglement island inevitably disappears, thus leading to a short-time information paradox.

International Conference on Particle Physics and Cosmology (ICPPCRubakov2023)
02-07, October 2023
Yerevan, Armenia

*Speaker

PoS(ICPPCRubakov2023)040

1. Introduction

Black holes and their radiation, continue to be enigmatic and mystifying phenomena [1, 2]. Typically the textbook version of information paradox is formulated in terms of mixed/pure state transition. Another formulation refers to the entanglement entropy content of the fields surrounding the black hole. For example for four dimensional black hole the paradox manifests itself when we consider infinite regions containing spatial infinity on both sides of maximally extended version of such black hole. The entanglement entropy of these regions increases during the time evolution and after some time exceeds the black hole entropy itself.

To save the unitarity which is violated in the situation being just described the series of papers [5–9] introduced a so-called entanglement islands (or island mechanism) stopping the entanglement growth. This mechanism has its roots in the requirement that the path integral geometry generating the reduced density matrix corresponding to the certain entanglement region I under consideration (i.e. original geometry plus slits along the this I) should be consistent with the gravitational equations of motion. Consequences of these considerations, entanglement islands and their effect on quantum information dynamics has been studied in different versions and setups, for example in two-dimensional gravity [5–13] and in moving mirrors [14, 15]. The origin of entanglement modification for dynamical gravity is hidden in special class of wormhole solutions elusively present in the entanglement entropy calculation when the dynamical gravity is turned on [6–13]. This could be viewed in fact in some sense as a far-looking implication of the pioneering paper by Valery Rubakov, George Lavrelashvili and Peter Tinyakov [16] devoted to the loss of coherence due to presence of wormhole-like contributions (however, instead of breaking coherence replica wormholes save it generating island phenomena). These objects will be renowned as baby-universe in what follows in this context [17, 18].

Rigorous arguments in favor of entanglement islands are accessible in a straightforward manner in lower-dimensional models, while in higher-dimensional setup our possibilities to study this class of problems are quite restricted. One of the possibilities is to use the s-wave approximation i.e. effectively reduce higher-dimensional setup to lower dimensional one and assume the existence of islands in a similar form as in the lower-dimensional models. This was done in [19] and generalized in different contexts recently for different setups [20–34].

In this contribution, we consider the following question: what happens with information paradox, entanglement islands in the s-wave approximation if we confine Hawking radiation in each (left and right) exterior of eternal black hole with the perfectly reflecting boundary.

Placing black hole in a cavity is a classical way to understand a wide range of phenomena related to them – this introduces a new scale at the spatial infinity, regulates a possible divergences related to infinities etc. [35, 36]. As an example of importance of infrared modes in the context of entanglement islands see [33].

We find that the introduction of the cavity leads to the significant qualitative behaviour of the entanglement entropy evolution and island islands – in the absence of entanglement islands one can find locations of boundaries without information paradox. On the other hand we find that now the entanglement islands literally does not work unavoidably disappearing for some restricted time. This paper is largely based on [37].

The paper is organized as follows. In section 2, we setup the notation, present out path-integral geometries and remind basic formulae from BCFT. Section 3 is devoted to the entanglement entropy dynamics and we introduce blinking island effect in it. Final section is devoted to conclusions.

2. Setup

Entanglement entropy of matter in BCFT$_2$

Boundary conformal field theory (BCFT) is the analog of ordinary conformal field theory but with the presence of boundaries. The simplest boundary field theory in two-dimensions is the theory defined on upper half-plane (UHP). Denoting x_1 coordinate the Euclidean time and x_2 is the spatial coordinate we define the metric

$$ds^2 = dx_1^2 + dx_2^2 = dzd\bar{z}, \quad z = x_1 + ix_2, \quad x_1 \in (-\infty, \infty), \quad x_2 \geq 0, \tag{1}$$

The region R we are interested in consists of union of intervals

$$R = [z_{a_1}, z_{b_1}] \cup \ldots \cup [z_{a_n}, z_{b_n}], \tag{2}$$

and the entanglement entropy $S_{\rm m}(R) = -\operatorname{Tr}(\rho_R \log \rho_R)$ is defined via resuced density matrix ρ_R corresponding to the region R. Entanglement entropy is given [38, 39] as the limit $S_{\rm m}(R) = -\lim_{n\to 1} \partial_n \left(\operatorname{Tr} \rho_R^n\right)$ with the trace being expressed as the certain correlation of primary operators with conformal dimension $h_n = \bar{h}_n = c/24(n - 1/n)$ – twist operators[1] inserted at the endpoints of region R (called entangling interval or entangling region).[2] Explicilty one can express the trace as the correlation function

$$\operatorname{Tr} \rho_R^n = \langle \phi(z_{a_1}, \bar{z}_{a_1}) \phi(z_{b_1}, \bar{z}_{b_1}) \ldots \phi(z_{a_n}, \bar{z}_{a_n}) \phi(z_{b_n}, \bar{z}_{b_n}) \rangle_{\rm UHP}. \tag{3}$$

We consider two-dimensional BCFT consisting of c copies of two-dimensional free massless Dirac fermions in curved spacetime with the boundary conditions preserving the conformal invariance [40–42]. For such a theory the entanglement entropy of region (2) is given by [43, 44]

$$\begin{aligned} S(R) =& \frac{1}{3} \sum_{i,j=1}^{n} \log |z_{a_i} - z_{b_j}| - \frac{1}{3} \sum_{i<j}^{n} \log |z_{a_i} - z_{a_j}||z_{b_i} - z_{b_j}| - n \log \varepsilon \\ &+ \frac{1}{6} \sum_{i,j=1}^{n} \log |z_{a_i} - \bar{z}_{a_j}||z_{b_i} - \bar{z}_{b_j}| - \frac{1}{6} \sum_{i,j=1}^{n} \log |z_{a_i} - \bar{z}_{b_j}||z_{b_i} - \bar{z}_{a_j}|, \end{aligned} \tag{4}$$

where ε is UV cutoff.

Under conformal transformation $z = z(w)$ correlation function of primary operators on UHP transforms as

$$\begin{aligned} \langle \phi(w_1, \bar{w}_1) \ldots \phi(w_m, \bar{w}_m) \rangle_\Omega = \prod_{j=1}^{m} \left(\frac{dz}{dw}\right)^{h_n} \Big|_{w=w_j} \left(\frac{d\bar{z}}{d\bar{w}}\right)^{\bar{h}_n} \Big|_{\bar{w}=\bar{w}_j} \\ \times \langle \phi(z_1, \bar{z}_1) \ldots \phi(z_m, \bar{z}_m) \rangle_{\rm UHP}. \end{aligned} \tag{5}$$

[1] Here c is the central charge.

[2] Each endpoint should not belong to the boundary.

From a similar property following from the Weyl trasnformation property of primary operators for transition between metric $ds^2 = dwd\bar{w} \to ds^2 = e^{2\rho(w,\bar{w})}dwd\bar{w}$ entanglement entropy changes as

$$S_{\rm m}\Big|_{ds^2=e^{2\rho(w,\bar{w})}dwd\bar{w}} = S_{\rm m}\Big|_{ds^2=dwd\bar{w}} + \frac{c}{6}\sum_{i=1}^{m}\log e^{\rho(w_i,\bar{w}_i)}. \tag{6}$$

Following s-wave approximation from [19] for geometries of the form

$$ds^2 = e^{2\rho(w,\bar{w})}dwd\bar{w} + r^2 d\Omega_d^2, \tag{7}$$

we effectively neglect the spherical part of the metric $d\Omega_d^2$ and consider two-dimensional BCFT on background

$$ds^2 = e^{2\rho(w,\bar{w})}dwd\bar{w}. \tag{8}$$

As in [19] we assume that the obtained results in such approximation captures all main features of dynamics in the original backgroun in higher dimensions.

Geometry, introduction of the boundaries and path-integral

The geometry of interest is given by the metric of the four-dimensional Schwarzschild black hole

$$ds^2 = -f(r)dt^2 + \frac{dr^2}{f(r)} + r^2 d\Omega_2^2, \qquad f(r) = 1 - \frac{r_h}{r}, \tag{9}$$

at $r > r_h$, $-\infty < t < \infty$, where $r_h = 2GM$ denotes the black hole horizon, M is the mass of the black hole, G is the gravitational constant and $d\Omega_2^2$ is the angular part of the metric. We consider only the two-dimensional part of the metric (9) relying on the s-wave approximation described above and within its framework omitting the angular variables in Kruskal coordinates

$$U = -\frac{1}{\kappa_h}e^{-\kappa_h(t-r_*(r))}, \quad V = \frac{1}{\kappa_h}e^{\kappa_h(t+r_*(r))}, \quad \kappa_h = 1/2r_h, \tag{10}$$

we are left with the two-dimensional metric of the form

$$ds^2 = -e^{2\rho(r)}dUdV, \quad e^{2\rho(r)} = f(r)e^{-2\kappa_h r_*(r)}, \tag{11}$$

where $r_*(r)$ is tortoise coordinate given by $r_*(r) = r + r_h\log|r - r_h|/r_h$. It is convenient now to relate Kruskal coordinates to timelike T and spacelike X variables

$$U = T - X, \qquad V = T + X, \tag{12}$$

expressed in terms of Schwarzschild coordinates as

$$T = \pm\frac{e^{\kappa_h r_*(r)}}{\kappa_h}\sinh\kappa_h t, \qquad X = \pm\frac{e^{\kappa_h r_*(r)}}{\kappa_h}\cosh\kappa_h t, \tag{13}$$

where the upper (lower) sign corresponds to the right (left) wedge. We Wick rotate Kruskal time $T = -i\mathcal{T}$ and this also defines the Euclidean Schwarzschild time $\tau = it$ periodic with a period of $2\pi/\kappa_h$. The coordinate transformation (13) now takes the form

$$\mathcal{T} = \pm\frac{e^{\kappa_h r_*(r)}}{\kappa_h}\sin\kappa_h\tau, \qquad X = \pm\frac{e^{\kappa_h r_*(r)}}{\kappa_h}\cos\kappa_h\tau. \tag{14}$$

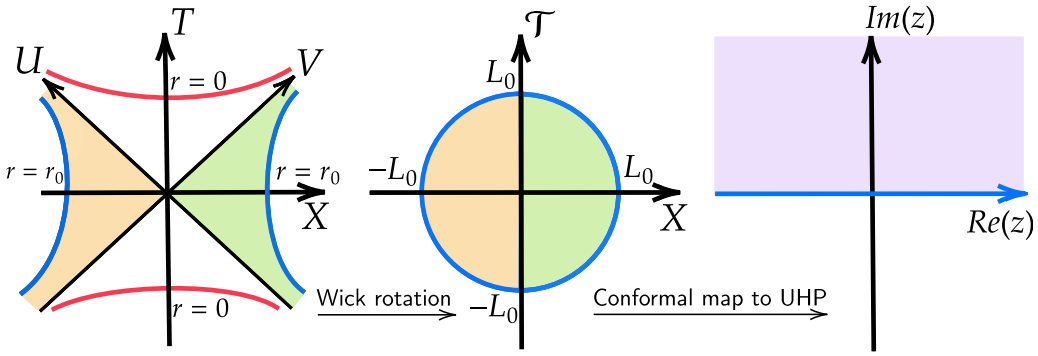

Figure 1: Lorentzian (**left**) and Euclidean (**center**) Kruskal diagram of a two-sided Schwarzschild black hole in the presence of two symmetric boundaries at $r = r_0$ drawn in blue. The Euclidean Kruskal diagram corresponds to the interior of the disk, that maps conformally to the upper half-plane (**right**).

and left (right) half-plane $X < 0$ ($X > 0$) corresponds to the left (right) wedge of Lorentzian black hole. It is straightforward to see that in the $(\mathcal{T}, X)$ plane curves $r = \text{const}$ correspond to circles centered at the point $\mathcal{T} = X = 0$ and $\tau = \text{const}$ to the straight lines passing through this point. We consider the exterior of the Euclidean black hole, i.e. $r \geq r_h$, and the origin of the $(\mathcal{T}, X)$ plane corresponds to $r = r_h$.

Introducing a complex coordinates

$$w = X + i\mathcal{T}, \qquad \bar{w} = X - i\mathcal{T}, \tag{15}$$

we get the Euclidean version of the metric (11) in the form

$$ds^2 = e^{2\rho(w,\bar{w})} dw d\bar{w}, \qquad e^{2\rho(w,\bar{w})} = \frac{W(e^{-1}\kappa_h^2 w\bar{w})}{\kappa_h^2 w\bar{w}\left[1 + W(e^{-1}\kappa_h^2 w\bar{w})\right]}, \tag{16}$$

where $W(x)$ is Lambert W function. Total geometry given by (16) (i.e. at $-\infty < \mathcal{T}, X < \infty$) is just the complex plane endowed with the non-trivial metric. Spherically symmetric boundary is located at the radial coordinate $r = r_0$, where $r_0 > r_h$, in the analytically extended Schwarzschild geometry. Two boundaries both in the right and left wedges are located at the same radial coordinate. The Euclidean geometry in the plane $(\mathcal{T}, X)$ corresponds to the interior of a disk with the radius $L_0 = e^{\kappa_h r_*(r_0)}/\kappa_h$, see Fig.1. Quantum fields (Dirac fermions) now are restricted by the boundary at $r < r_0$ via reflecting boundary condition being imposed. So from the path-integral point of view the wavefunctional of our interest is given by the integration over the geometry part with $\mathcal{T} < 0$, i.e. over the lower half of the disk from Fig.1.

The next step is to perform conformal mapping of the Euclidean geometry given by the central picture in Fig.1 to the upper half-plane with non-trivial curved metric and then implement Weyl transformation to the flat metric upper half-plane. In this way we obtain explicit form of the entanglement entropy given by the composition of transformation rules for conformal mappings (5) and Weyl transformations (6). The map from the interior of the disk with radius L_0 to the UHP is

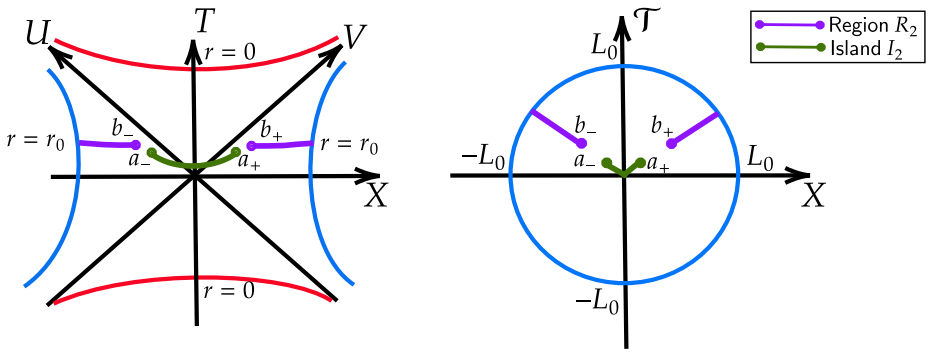

Figure 2: The schematic depicture of the region R_2 (magenta) in: two-boundary Lorentzian geometry (**left**) and its Euclidean version (**right**).

defined by

$$z = i\frac{L_0 + w}{L_0 - w}, \qquad \bar{z} = -i\frac{L_0 + \bar{w}}{L_0 - \bar{w}}. \tag{17}$$

Generalized entropy functional

The reduced density matrix of Hawking radiation collected in R is defined by tracing out the states in the complement region $\overline{R}$, which includes the black hole interior. The island mechanism prescribes that the states in some regions $I \subset \overline{R}$, called entanglement islands, are to be excluded from tracing out.

The island contribution can be taken into account via the generalized entropy functional defined as [8, 9]

$$S_{\rm gen}[I, R] = \frac{\text{Area}(\partial I)}{4G} + S_{\rm m}(R \cup I). \tag{18}$$

Here ∂I denotes the boundary of the entanglement island, G is Newton's constant, and $S_{\rm m}$ is the entanglement entropy of conformal matter. One should extremize this functional over all possible island configurations

$$S^{\rm ext}_{\rm gen}[I, R] = \operatorname*{ext}_{\partial I} \Big\{ S_{\rm gen}[I, R] \Big\}, \tag{19}$$

and then choose the minimal one.

3. Entanglement entropy in eternal black hole in the presence of reflecting walls

Let us calculate the entanglement entropy of the region R_2, which is the union of two intervals located between bulk points $\mathbf{b}_\pm$ and the boundary in the corresponding left/right wedge (magenta curves in Fig.2). In the island phase we assume the inclusion of the island region I_2 given by the "interval" between two points $\mathbf{a}_-$ and $\mathbf{a}_+$ in different wedges (green curves in Fig.2)

Entanglement entropy without island contribution

Here we study the entanglement entropy without island phase and explicitly choose the points $\mathbf{b}_\pm$ as

$$\mathbf{b}_+ = (r_b, t_b)\,, \qquad \mathbf{b}_- = (r_b, -t_b)\,. \tag{20}$$

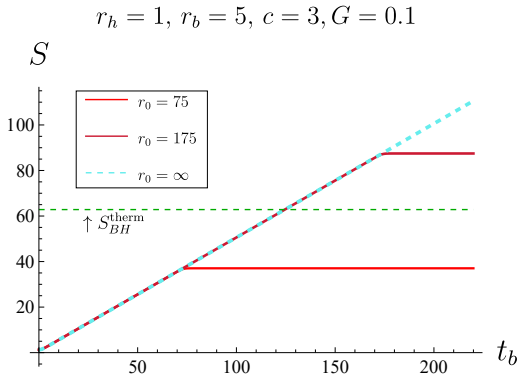

Figure 3: Time dependence of entanglement entropy without an island (21) for different boundary positions without taking into account entanglement islands. The entropy saturation time increases with the increase of boundary location r_0.

With this choice of points after some algebra one writes down the time-dependent entanglement entropy of R_2 as

$$S(R_2) = \frac{c}{6}\log\left(\frac{4f(b)\cosh^2\kappa_h t_b}{\kappa_h^2\varepsilon^2}\right) + \frac{c}{6}\log\left(\frac{2\sinh^2\kappa_h(r_*(r_0)-r_*(r_b))}{\cosh 2\kappa_h(r_*(r_0)-r_*(r_b))+\cosh 2\kappa_h t_b}\right). \tag{21}$$

Note that in the limit $r_0 \to \infty$ the second term of (21) tends to zero leading to infinite growth of entanglement. The time dependence of the entanglement entropy (21) for different positions of the boundary r_0 and the comparison with the entanglement entropy for the case without boundaries (i.e. at $r_0 \to \infty$) are shown in Fig. 3.

Blinking island effect – island disappears for some time

Now let use the formula (18) and observe how the entanglement entropy evolution is changed due to the presence of islands. Due to the symmetric choice of endpoints $\mathbf{b}_\pm$ (20) of the region R_2 and the symmetrical location of boundaries in both wedges, it follows that the endpoints $\mathbf{a}_\pm$ of island I_2 are also symmetric and are given as follows

$$\mathbf{a}_+ = (r_a, t_a)\,, \qquad \mathbf{a}_- = (r_a, -t_a)\,, \tag{22}$$

where the point $\mathbf{a}_+$ ($\mathbf{a}_-$) is located in the right (left) wedge. The generalized entropy (18) with the symmetric island I_2 is

$$S_{\text{gen}}[I_2, R_2] = S_I^{\text{wb}}(R_2) + S_I^{\text{b}}(R_2), \tag{23}$$

where the first term $S_I^{\text{wb}}(R_2)$ is independent of radial coordinate r_0 of boundary. In the limit $r_0 \to \infty$ we are left only with this term corresponding to the generalized entropy for a two-sided black hole with regions extending to spacelike infinity [19]

$$\begin{aligned} S_I^{\text{wb}}(R_2) = \frac{2\pi r_a^2}{G} &+ \frac{c}{3}\log\left(\frac{4\sqrt{f(r_a)f(r_b)}\cosh\kappa_h t_a\cosh\kappa_h t_b}{\kappa_h^2\varepsilon^2}\right) \\ &+ \frac{c}{3}\log\left(\frac{\cosh\kappa_h(r_*(r_a)-r_*(r_b)) - \cosh\kappa_h(t_a-t_b)}{\cosh\kappa_h(r_*(r_a)-r_*(r_b)) + \cosh\kappa_h(t_a+t_b)}\right). \end{aligned} \tag{24}$$

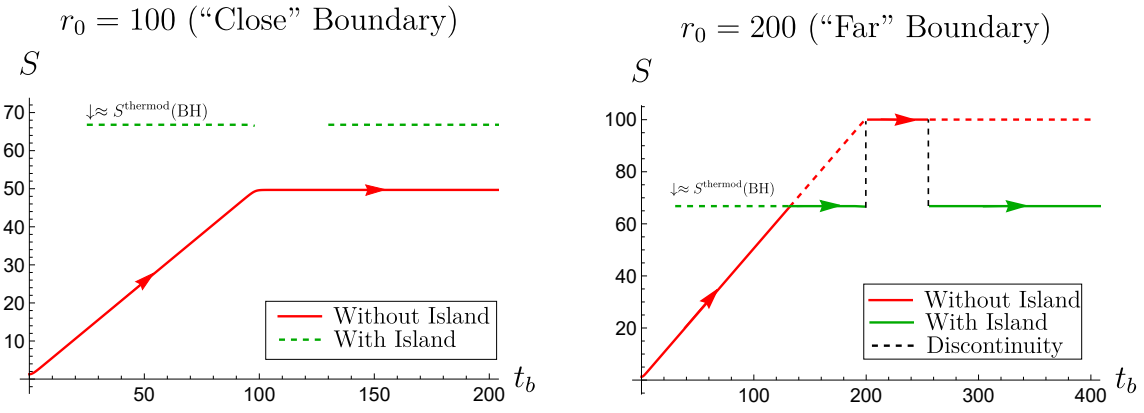

Figure 4: Time dependence of entanglement entropy taking into account nontrivial island configuration for a black hole with symmetric boundary for different boundary locations r_0. For $r_0 = 100$ we see that no islands are needed to avoid information paradox (red line is below the gren one), while for $r_0 = 200$ we see instantaneous transition to red line from green one and the back – i.e. island is switched of and information paradox is present for some time period.

The second term of generalized entropy (23) is the contribution purely due to the boundary inclusion

$$S_I^{\text{b}}(R_2) = \frac{c}{3}\log\left(\frac{\cosh\kappa_h(2r_*(r_0) - r_*(r_b) - r_*(r_a)) + \cosh\kappa_h(t_a + t_b)}{\cosh\kappa_h(2r_*(r_0) - r_*(r_b) - r_*(r_a)) - \cosh\kappa_h(t_a - t_b)}\right)$$
$$+ \frac{c}{6}\log\left(\frac{4\sinh^2\kappa_h(r_*(r_0) - r_*(r_a))\sinh^2\kappa_h(r_*(r_0) - r_*(r_b))}{(\cosh 2\kappa_h(r_*(r_0) - r_*(r_a)) + \cosh 2\kappa_h t_a)(\cosh 2\kappa_h(r_*(r_0) - r_*(r_b)) + \cosh 2\kappa_h t_b)}\right). \tag{25}$$

In accordance with the prescription of the island formula, it is necessary to carry out extremization with respect to the radial and time coordinates (r_a, t_a) of the island boundaries in (23), i.e. find the solutions of

$$\begin{cases}\partial_{r_a} S_{\text{gen}}[I_2, R_2]\,(r_a, t_a, r_b, t_b, r_0, r_h, c, G) = 0,\\ \partial_{t_a} S_{\text{gen}}[I_2, R_2]\,(r_a, t_a, r_b, t_b, r_0, r_h, c, G) = 0.\end{cases} \tag{26}$$

We consider solutions to the system (26) corresponding to the location of the island boundary r_a near the horizon, i.e. $r_a = r_h + X$, $X/r_h \ll 1$. We also work within the framework of the condition $r_b \gg r_h$ (for the applicability of the s-wave approximation [19]) and also assuming $cG\kappa_h^2 \ll 1$.

The analysis of the system (26) has been performed in the paper [37] analytically and numerically (it is quite cumbersome and complicate, so we refer reader to this paper). The resulting evolution of the entanglement entropy could be summarized as follows (see Fig.4). One can observe, that in comparison with the island effect the entanglement entropy unavoidably leads to the time region, where the island solution does not exist. Thus, if we have the following situation. If the boundary is located close enough to the black hole horizon the entanglement cannot exceed its thermodynamical cousin, so we do not need any islands. However, if it is located faraway enough we meet the time region where the entanglement instantaneously blinks to the "no island" entanglement for some time, thus leading to information paradox.

4. Discussion and conclusion

In this paper we considered the effect of reflecting boundaries on the evolution of entanglement entropy of free massless Dirac fermions in the eternal black hole. We consider as the evolution of entanglement entropy without any entanglement islands, as well as taking their contribution into account. Also we use s-wave approximation thus effectively reducing four-dimensional problem of calculation of entanglement entropy to the two-dimensional one. Let us summarize our main findings

- The evolution of entanglement entropy without islands changes due to the presence of reflecting boundaries surrounding the black hole as follows. It follows mainly the same curve as for the entropy without boundaries, however, instead of infinite growth we observe saturation at some time moment (depending on how faraway boundary is located from horizon). Taking this into account for close enough boundary one can avoid information paradox (entanglement entropy does not exceed the thermodynamic one).
- In the absence of boundaries the entanglement islands saves the unitarity (in other words allow us to avoid information paradox). As we saw in the text above in the presence of boundaries the information paradox could be present for some locations of the boundary. However, one can show that in the presence of the boundaries (see Fig.4 the entanglement islands disappear a short time – thus leading to information paradox. We call this "blinking island effect".

Acknowledgments

This work is supported by the Russian Science Foundation (project 20–12–00200, Steklov Mathematical Institute).

References

[1] S. W. Hawking, "Particle Creation by Black Holes," Commun. Math. Phys. **43**, 199-220 (1975)

[2] S. W. Hawking, "Breakdown of Predictability in Gravitational Collapse," Phys. Rev. D **14** (1976), 2460-2473

[3] D. N. Page, "Information in black hole radiation," Phys. Rev. Lett. **71** (1993), 3743-3746 [arXiv:hep-th/9306083 [hep-th]].

[4] D. N. Page, "Time Dependence of Hawking Radiation Entropy," JCAP **09** (2013), 028 [arXiv:1301.4995 [hep-th]].

[5] G. Penington, "Entanglement Wedge Reconstruction and the Information Paradox," JHEP **09** (2020), 002 [arXiv:1905.08255 [hep-th]].

[6] A. Almheiri, N. Engelhardt, D. Marolf and H. Maxfield, "The entropy of bulk quantum fields and the entanglement wedge of an evaporating black hole," JHEP **12** (2019), 063 [arXiv:1905.08762 [hep-th]].

[7] A. Almheiri, R. Mahajan, J. Maldacena and Y. Zhao, "The Page curve of Hawking radiation from semiclassical geometry," JHEP **03** (2020), 149 [arXiv:1908.10996 [hep-th]].

[8] G. Penington, S. H. Shenker, D. Stanford and Z. Yang, "Replica wormholes and the black hole interior," JHEP **03** (2022), 205 [arXiv:1911.11977 [hep-th]].

[9] A. Almheiri, T. Hartman, J. Maldacena, E. Shaghoulian and A. Tajdini, "Replica Wormholes and the Entropy of Hawking Radiation," JHEP **05** (2020), 013 [arXiv:1911.12333 [hep-th]].

[10] A. Almheiri, R. Mahajan and J. Maldacena, "Islands outside the horizon," [arXiv:1910.11077 [hep-th]].

[11] H. Z. Chen, R. C. Myers, D. Neuenfeld, I. A. Reyes and J. Sandor, "Quantum Extremal Islands Made Easy, Part I: Entanglement on the Brane," JHEP **10** (2020), 166 [arXiv:2006.04851 [hep-th]].

[12] A. Almheiri, T. Hartman, J. Maldacena, E. Shaghoulian and A. Tajdini, "The entropy of Hawking radiation," Rev. Mod. Phys. **93** (2021) no.3, 035002 [arXiv:2006.06872 [hep-th]].

[13] H. Z. Chen, R. C. Myers, D. Neuenfeld, I. A. Reyes and J. Sandor, "Quantum Extremal Islands Made Easy, Part II: Black Holes on the Brane," JHEP **12** (2020), 025 [arXiv:2010.00018 [hep-th]].

[14] I. Akal, Y. Kusuki, N. Shiba, T. Takayanagi and Z. Wei, "Holographic moving mirrors," Class. Quant. Grav. **38**, no.22, 224001 (2021) [arXiv:2106.11179 [hep-th]].

[15] D. S. Ageev, "Shaping contours of entanglement islands in BCFT," JHEP **03** (2022), 033 [arXiv:2107.09083 [hep-th]].

[16] G. V. Lavrelashvili, V. A. Rubakov and P. G. Tinyakov, "Disruption of Quantum Coherence upon a Change in Spatial Topology in Quantum Gravity," JETP Lett. **46**, 167-169 (1987)

[17] S. B. Giddings and A. Strominger, "Loss of incoherence and determination of coupling constants in quantum gravity," Nucl. Phys. B **307**, 854-866 (1988)

[18] S. R. Coleman, "Black holes as red herrings: Topological fluctuations and the loss of quantum coherence," Nucl. Phys. B **307**, 867-882 (1988)

[19] K. Hashimoto, N. Iizuka and Y. Matsuo, "Islands in Schwarzschild black holes," JHEP **06** (2020), 085 [arXiv:2004.05863 [hep-th]].

[20] M. Alishahiha, A. Faraji Astaneh and A. Naseh, "Island in the presence of higher derivative terms," JHEP **02**, 035 (2021) [arXiv:2005.08715 [hep-th]].

[21] Y. Ling, Y. Liu and Z. Y. Xian, "Island in Charged Black Holes," JHEP **03**, 251 (2021) [arXiv:2010.00037 [hep-th]].

[22] Y. Matsuo, "Islands and stretched horizon," JHEP **07**, 051 (2021) [arXiv:2011.08814 [hep-th]].

[23] G. K. Karananas, A. Kehagias and J. Taskas, "Islands in linear dilaton black holes," JHEP **03**, 253 (2021) [arXiv:2101.00024 [hep-th]].

[24] X. Wang, R. Li and J. Wang, "Islands and Page curves of Reissner-Nordström black holes," JHEP **04**, 103 (2021) [arXiv:2101.06867 [hep-th]].

[25] W. Kim and M. Nam, "Entanglement entropy of asymptotically flat non-extremal and extremal black holes with an island," Eur. Phys. J. C **81**, no.10, 869 (2021) [arXiv:2103.16163 [hep-th]].

[26] I. Aref'eva and I. Volovich, "A note on islands in Schwarzschild black holes," Teor. Mat. Fiz. **214**, no.3, 500-516 (2023) [arXiv:2110.04233 [hep-th]].

[27] S. He, Y. Sun, L. Zhao and Y. X. Zhang, "The universality of islands outside the horizon," JHEP **05**, 047 (2022) [arXiv:2110.07598 [hep-th]].

[28] I. Y. Aref'eva, T. A. Rusalev and I. V. Volovich, "Entanglement entropy of a near-extremal black hole," Teor. Mat. Fiz. **212**, no.3, 457-477 (2022) [arXiv:2202.10259 [hep-th]].

[29] W. C. Gan, D. H. Du and F. W. Shu, "Island and Page curve for one-sided asymptotically flat black hole," JHEP **07**, 020 (2022) [arXiv:2203.06310 [hep-th]].

[30] S. Azarnia and R. Fareghbal, "Islands in Kerr–de Sitter spacetime and their flat limit," Phys. Rev. D **106**, no.2, 026012 (2022) [arXiv:2204.08488 [hep-th]].

[31] A. Anand, "Page curve and island in EGB gravity," Nucl. Phys. B **993**, 116284 (2023) [arXiv:2205.13785 [hep-th]].

[32] D. S. Ageev and I. Y. Aref'eva, "Thermal density matrix breaks down the Page curve," Eur. Phys. J. Plus **137**, no.10, 1188 (2022) [arXiv:2206.04094 [hep-th]].

[33] D. S. Ageev, I. Y. Aref'eva, A. I. Belokon, A. V. Ermakov, V. V. Pushkarev and T. A. Rusalev, "Infrared regularization and finite size dynamics of entanglement entropy in Schwarzschild black hole," Phys. Rev. D **108**, no.4, 046005 (2023) [arXiv:2209.00036 [hep-th]].

[34] D. S. Ageev, I. Y. Aref'eva, A. I. Belokon, V. V. Pushkarev and T. A. Rusalev, "Entanglement entropy in de Sitter: no pure states for conformal matter," [arXiv:2304.12351 [hep-th]].

[35] J. W. York, Jr., "Black hole thermodynamics and the Euclidean Einstein action," Phys. Rev. D **33** (1986), 2092-2099

[36] D. J. Gross, M. J. Perry and L. G. Yaffe, "Instability of Flat Space at Finite Temperature," Phys. Rev. D **25**, 330-355 (1982)

[37] D. S. Ageev, I. Y. Aref'eva and T. A. Rusalev, "Black Holes, Cavities and Blinking Islands," [arXiv:2311.16244 [hep-th]].

[38] P. Calabrese and J. L. Cardy, "Entanglement entropy and quantum field theory," J. Stat. Mech. **0406** (2004), P06002 [arXiv:hep-th/0405152 [hep-th]].

[39] P. Calabrese and J. Cardy, "Entanglement entropy and conformal field theory," J. Phys. A **42** (2009), 504005 [arXiv:0905.4013 [cond-mat.stat-mech]].

[40] J. L. Cardy, "Conformal Invariance and Surface Critical Behavior," Nucl. Phys. B **240** (1984), 514-532

[41] J. L. Cardy, "Effect of Boundary Conditions on the Operator Content of Two-Dimensional Conformally Invariant Theories," Nucl. Phys. B **275** (1986), 200-218

[42] J. L. Cardy, "Boundary Conditions, Fusion Rules and the Verlinde Formula," Nucl. Phys. B **324** (1989), 581-596

[43] F. Rottoli, S. Murciano, E. Tonni and P. Calabrese, "Entanglement and negativity Hamiltonians for the massless Dirac field on the half line," J. Stat. Mech. **2301** (2023), 013103 [arXiv:2210.12109 [cond-mat.stat-mech]].

[44] J. Kruthoff, R. Mahajan and C. Murdia, "Free fermion entanglement with a semitransparent interface: the effect of graybody factors on entanglement islands," SciPost Phys. **11** (2021), 063 [arXiv:2106.10287 [hep-th]].